Indonesian Journal of Medical Laboratory Science and Technology
Open Access
p-ISSN 2684-6748
e-ISSN 2656-9825

RESEARCH ARTICLE

Computational modeling of a Novel CTX-M β-lactamase *Escherichia coli* isolated from Yogyakarta, Indonesia Using I-TASSER and SWISS-MODEL

Anggiresti Kinasih [1], Endah Retnaningrum [2]

[1]Laboratory Ecology and Biosystematics, Departement Biology, Faculty of Sains and Mathematics, Universitas Diponegoro, Semarang, Indonesia

[2]Laboratory of Microbiology, Department of Tropical Biology, Faculty of Biology, Universitas Gadjah Mada, Yogyakarta, Indonesia

Correspondence:
Endah Retnaningrum
Laboratory of Microbiology, Department of Tropical Biology, Faculty of Biology, Universitas Gadjah Mada, Yogyakarta – 55281, Indonesia

Email: endahr@ugm.ac.id

Article history:
Received: 2025-05-01
Revised: 2025-10-22
Accepted: 2026-03-11
Available online: 2026-03-30

Keywords:
Amino acid
Epidemic
Foodborne disease
Sequencing
Taxonomy

https://doi.org/10.33086/ijmlst.v8i1.7267

Abstract

Extended-spectrum β-lactamases (ESBLs), particularly those of the CTX-M family, play a critical role in mediating antibiotic resistance in *Escherichia coli*. While CTX-M variants have been widely reported in clinical isolates, their genetic and structural diversity in foodborne *E. coli* from Indonesia remains poorly characterized. To address this gap, a single *E. coli* isolate (D4DU2-ESBL-EC) was selected. Genomic DNA was extracted and sequenced to obtain the complete nucleotide sequence. Furthermore, a total of 23 reference sequences from all of the CTX-M variant groups in Enterobacteriaceae were selected from NCBI. Phylogenetic reconstruction was carried out with MEGA11, and haplotype network analysis was conducted with DnaSP. Additionally, amino acid sequence comparisons were performed to assess the novelty of the D4DU2-ESBL-EC isolate. Three-dimensional (3D) structure modeling was generated using the C-I-TASSER (Iterative Threading ASSEmbly Refinement) server and SWISS-MODEL for comparison. Structural validation was performed using the Structure Validation Server (SAVES v6.1) and MolProbity. The phylogenetic and haplotype analyses revealed that D4DU2-ESBL-EC is evolutionarily closest to *E. coli* CTX-M-15 but carries two amino acid substitutions (W253L and P254A) located near the enzyme's active site. This suggests a potentially novel CTX-M variant. The predicted 3D model exhibited high stereochemical quality, with 78.4% of residues in the most favored regions and 20.5% in allowed regions. Based on these findings, it can be concluded that *E. coli* D4DU2-ESBL-EC represents a new CTX-M variant isolated from foodborne samples in Yogyakarta, Indonesia, closely related to blaCTX-M-15 variants reported in India.

1. INTRODUCTION

Escherichia coli is a Gram-negative bacterium of concern because it is associated with serious foodborne illnesses, particularly when it carries antibiotic resistance genes (1). Notably, pathogenic *E. coli* strains pose a public health risk as they can to contaminate food products (2), especially raw meat, and cause various gastrointestinal illnesses (3,4). Among its resistance mechanisms, one of the most concerning in *E. coli* is the production of extended-spectrum β-lactamases (ESBLs) (5). These enzymes provide resistance to a wide range of β-lactam antibiotics, including penicillins and cephalosporins (6). Sudarwanto et al. (7) first reported CTX-M-producing *E. coli* in Indonesia, detecting CTX-M-1 and CTX-M-55 variants in broiler feces from a slaughterhouse in Bogor, West Java. CTX-M β-lactamase, a prominent ESBL subclass, has attracted global attention for its rapid spread and clinical significance. According to Saliu et al. (8), misuse of antibiotics in poultry, including use as growth promoters, accelerates the selection of ESBL-producing bacteria. This poses a public health concern, as ESBL-producing *E. coli* can transfer resistance genes to other bacteria, in both animals and humans, through horizontal gene transfer (9).

Citation: Kinasih A, Retnaningrum E. Computational modeling of a Novel CTX-M β-lactamase *Escherichia coli* isolated from Yogyakarta, Indonesia Using I-TASSER and SWISS-MODEL. Indones J Med Lab Sci Technol. 2026;8(1):55–66. https://doi.org/10.33086/ijmlst.v8i1.7267

In Indonesia, CTX-M β-lactamase-producing *E. coli* has been found in hospitals and food sources (10). However, data about the prevalence and molecular diversity of CTX-M variants, especially those from traditional food markets, remain scarce. Several CTX-M types, such as CTX-M-15, are highly virulent and fluoroquinolone resistant (11). CTX-M β-lactamase circulates in Indonesia and spreads among chickens in Tangerang (12), healthy residents in Lombok (13), dairy farms in East Java (14), and hospital patients in Pontianak, West Kalimantan (15). Nevertheless, information on newer or less common variants of CTX β-lactamase-producing *E. coli*, particularly in raw meat from traditional markets, remains limited, and few studies have investigated these at the proteomic level.

The β-lactamase enzymes require 3D structural simulations to elucidate their function and catalytic mechanisms, thus facilitating the discovery of novel inhibitors. The 3D structure of proteins or enzymes can be determined using advance instruments, such as X-ray crystallography, nuclear magnetic resonance (NMR) spectroscopy, and cryogenic electron microscopy (cryo-EM) (16). While the 3D structures obtained by these methods are high-resolution, each technique has limitations. For example, X-ray crystallography requires crystallization of the enzyme, a challenging and time-intensive process (17). In contracts, NMR spectroscopy allows stereochemical visualization of small-molecule enzymes, but demands specific samples sizes and precise concentration ranges (18). Meanwhile, cryo-EM can resolve large protein complexes, but it is costly and requires highly skilled personnel (19).

Developing an *in-silico* approach offers a more efficient and cost-effective alternative to using heavy equipment to construct enzyme 3D structures. Specifically, with *in silico* approaches, the novel CTX β-lactamase 3D structure can be visualized by integrating template threading, fragment assembly, and atomic-level refinement with I-TASSER (Iterative Threading Assembly Refinement) (20). Furthermore, the stereochemical quality of these visualized enzymes can then be validated using Ramachandran plots and geometric parameter analysis with PROCHECK (21). Additionally, *in silico* tools such as molecular docking can assess whether specific mutations and amino acid substitutions in the CTX β-lactamase active site affect interactions with antibiotics and may indicate possible changes in inhibitor susceptibility (22).

Molecular probes can be used computationally to investigate structural and functional changes caused by mutations in a novel β-lactamase. These probes reveal effects on inhibitory mechanisms (23). Avibactam is the most effective inhibitor of class A and C β-lactamase. It is a useful as a molecular probe, especially for CTX-M enzymes (24). Avibactam forms reversible covalent bonds with the catalytic serine residue. This allows repeated inhibition cycles without hydrolysis, unlike traditional antibiotic such as clavulanic acid or tazobactam (25).

Although *in silico* analysis has become more common globally, its application to predict ESBL enzyme structures and their roles in the spread of CTX-M β-lactamase-producing *E. coli* through the food chain in Indonesia remains underexplored. This study addresses this gap by predicting and validating the 3D structure of a novel CTX-M β-lactamase from *E. coli* D4DU2-ESBL-EC isolated in Yogyakarta, Indonesia, using I-TASSER and PROCHECK (26). Identifying this new CTX-M variant will provide essential structural data on ESBL, strengthen food safety surveillance, and inform strategies to reduce the risk of antibiotic-resistant bacteria spreading in Indonesia.

2. MATERIALS AND METHODS

2.1. Study Period and Location

The laboratory experiments and computational analysis were conducted over 1,5 years, from April 2023 to July 2024, at the Microbiology Laboratory, Faculty of Biology, Universitas Gadjah Mada (Yogyakarta, Indonesia). Validation of the results and data analysis were carried out separately in the Ecology and Biosystematics Laboratory, Faculty of Science and Mathematics, Universitas Diponegoro (Semarang, Indonesia), from August 2024 to May 2025.

2.2. Bacterial Isolate and Gene Source

A culture collection from the Microbiology Laboratory at Universitas Gadjah Mada (Yogyakarta, Indonesia), provided the *E. coli* strain (D4DU2-ESBL-EC) used in this study. Originally, this strain was isolated from broiler chicken breast meat collected at a traditional market in Yogyakarta. Its identity as an ESBL-producing *E. coli* was confirmed through morphological, biochemical, and phenotypic screening, followed by molecular confirmation. Genomic DNA was extracted for the blaCTX-M gene using standard microbiological and molecular procedures. The resulting blaCTX-M amplicon was purified, submitted for Sanger sequencing at 1st Base Laboratory (Singapore), and the resulting sequence was analyzed using BLASTn (27).

2.3. Phylogenetic Analysis of CTX-M Gene Variants

To evaluate the novelty of the blaCTX-M gene in isolate D4DU2 ESBL-EC and determine the evolutionary relationship of the CTX-M gene, a phylogenetic tree was constructed using representative sequences of different CTX-M variants retrieved from the NCBI GenBank database. Reference sequences included representatives from the CTX-M-1, CTX-M-9, CTX-M-14, CTX-M-15, CTX-M-25, CTX-M-27, CTX-M-65, and CTX-M-123 groups. These reference sequences were selected in FASTA format to cover the major CTX-M families known for extended-spectrum β-lactamase (ESBL) activity in Enterobacteriaceae. Multiple sequence alignment was performed using the MUSCLE algorithm (28) in MEGA11 software

(v11.0.13, https://www.megasoftware.net) (29). Phylogenetic reconstruction was conducted using the Maximum Likelihood (ML) method with 1,000 bootstrap replicates to provide reliable data. Tamura's 3-parameter nucleotide substitution model was used with a gamma distribution (+G = 1.07) to account for rate heterogeneity among sites (30). Pairwise genetic distances and topology visualization were used for evolutionary analysis, determining the genetic affiliation of *E. coli* D4DU2 and its potential clustering with other known CTX-M variants within the resistance group.

2.4. Amino Acid Substitution and Haplotype Network Analysis

The D4DU2-ESBL-EC DNA sequence was translated into an amino acid sequence with the Expasy Translate tool to analyze the physicochemical properties of CTX β-lactamase enzymes. The amino acid sequence of *E. coli* D4DU2 was aligned with reference CTX-M variants (CTX-M-1, -9, -14, -15, -25, -65, and -123) using BioEdit v7.7.1.0 to analyze conserved serine hydrolase sequences in ESBLs and to detect specific mutations. To assess allelic diversity and identify potential common ancestors among CTX-M variants, haplotype analysis was performed with DnaSP v6.0, outputting results in NEXUS or FASTA formats (31). The NEXUS file was then used to construct a haplotype network using the median-joining algorithm NETWORK v10.2.0.0 (Fluxus Technology Ltd., UK) (34). In the haplotype visualization, nodes represent unique haplotypes, their size reflects frequency, and edges show the number of mutations between closely related isolates. The resulting network provided a comprehensive visualization of genetic distances and potential mutational pathways linking *E. coli* D4DU2 to other CTX-M lineages.

2.5. Structural Modeling and Validation of CTX-M Enzyme

Subsequently, the three-dimensional structure of the CTX-M enzyme was predicted using the C-I-TASSER (Iterative Threading ASSEmbly Refinement) server. The resulting model was directly compared with that generated by SWISS-MODEL (33). The 199-residue protein domain was then submitted for structural modeling. C-I-TASSER builds structures through multiple threading alignments and iterative fragment assembly. Parameters for the C-I-TASSER model included a C-score of 1.71, a TM-score of 0.95 ± 0.05, and a RMSD of 2.0 ± 1.6 Å. The high TM-score indicates reliability and high similarity to experimentally solved structures, as described by Zheng et al. (34) and Yang et al. (35). The three-dimensional model of lactamase protein was subsequently visualized using PyMOL (v2.5.0) (36) and Discovery Studio Visualizer (v21.1.0) (37). Its quality was then validated using the Structure Validation Server (SAVESv6.1) by analyzing the Ramachandran plot (38), where a reliable model was defined by having more than 90% of residues in the most favored regions. Finally, Molprobity was used as additional validation for the protein model (39).

2.6. Structural Comparison with Reference CTX-M Protein

A reference structure from the Protein Data Bank (PDB) was selected for comparison with the modeled CTX-M variant. Specifically, PDB ID: 7TI0, which represents a clinically relevant CTX-M-15-type beta-lactamase from *E. coli*, served as the comparative template. Before alignment and structural analysis, non-standard amino acids and the native ligand were removed from 7TI0 in UCSF Chimera, retaining only the protein backbone for conformational analysis. The 3D structure alignment of D4DU2-ESBL-EC with the 7T10 backbone was then performed in PyMol to highlight unique features, mutations, and active-site regions.

2.7. Functional Analysis of D4DU2-ESBL-EC Active Site Mutations by Molecular Docking

Molecular docking was performed using an *in-silico* approach to evaluate whether the predicted protein confers antibiotic resistance, particularly in relation to the identified mutations (W253L and P254A). The three-dimensional (3D) structures of various antibiotics were retrieved from PubChem (https://pubchem.ncbi.nlm.nih.gov/) in .sdf format (40). The 3D structure of the reference protein was obtained from C-I-TASSER prediction, which identified PDB templates 1IYP and 3BFC as the closest structural homologs to D4DU2-ESBL-EC, exhibiting similar binding sites with C-scores of 0.91 and 0.88, RMSD values of 0.90 and 0.91, and sequence identities of 83% and 71%, respectively. The 1IYP structure represents Toho-1 β-lactamase derived from *E. coli*, while 3BFC corresponds to a class A β-lactamase from *E. coli* BL21. Both serve as wild-type reference proteins, and both 3D structures were collected from RCSB PDB (41). According to the protein database, both template structures contain naturally bound ligands, referred to as native ligands; protein 1IYP is complexed with cephalothin, and protein 3BFC is complexed with imipenem. Therefore, redocking was performed to compare the binding energies between the native ligands and the tested compounds. Protein preparation was conducted using UCSF Chimera 1.17.3 (42) to remove all non-standard amino acids, followed by AutoDockTools 1.5.6 (43) to assign Gasteiger charges, remove water molecules, add hydrogen atoms, and define AD4 atom types. Molecular docking simulations were carried out using PyRx, and only binding affinities with an RMSD value ≤2Å were reconsidered (44). In the docking, three independent replicates were performed, and the resulting binding affinity values were analyzed using two-way ANOVA to determine statistical significance. Docking validation was performed in PyMOL. The resulting complexes were saved in .pdb format and subsequently visualized using Discovery Studio to analyze the binding pockets and amino acid residues involved in the inhibitory activity of the β-lactamase enzyme.

3. RESULTS AND DISCUSSION

The emergence of ESBL bacterial variants is a major health concern, especially when they are found in raw food products such as chicken meat. This relates to bacteria's ability to carry out gene transfer. When resistant genes are transferred to pathogenic bacteria, they can cause serious infectious diseases that are difficult to cure due to antibiotic-resistance (45). Detection of *E. coli* CTX-M variants among ESBL strain will help in understanding and monitoring the epidemiology of an infectious disease. The *E. coli* D4DU2-ESBL-EC isolate was selected for further analysis because it carries the *bla*CTX-M gene, exhibits phenotypic multidrug resistance to CAZ, CTX, and ATM, and is sensitive AMC. Strains carrying the *bla*CTX-M gene are more likely to hydrolyze cefotaxime as a beta-lactam antibiotic (46).

3.1. Phylogenetic Reconstruction of *Escherichia coli* CTX-M Variants

As shown in Figure 1, the blaCTX-M sequence from the D4DU2-ESBL-EC isolate clustered within the *E. coli* CTX-M-15 lineage. It formed a monophyletic branch with a high bootstrap value of 72%. This close evolutionary proximity indicates high sequence similarity and a probable shared ancestor of D4DU2-ESBL-EC with CTX-M-15. Further molecular characterization is needed to verify if D4DU2-ESBL-EC represents a new variant, as there is no significant divergence or clear branch separation between D4DU2-ESBL-EC and CTX-M-15.

The topology also revealed a monophyletic group with moderate to high support bootstrap (78% to 100%), including CTX-M-9/14/13/27/65, which is closely related to CTX-M-123 and distant from another subclade, CTX-M-8/25. The segregation between CTX-M variants reflects a clear phylogenetic divergence between the CTX-M-1-type group (to which CTX-M-15 and blaCTX-M D4DU2-ESBL-EC belong) and the CTX-M-9-type group, consistent with previously reported evolutionary classifications (47). Supporting evidence from Yu et al. (48) demonstrates a close genetic relationship between $bla_{CTX\text{-}M\text{-}1}$ and $bla_{CTX\text{-}M\text{-}15}$, driven by the presence of the IS*Ecpl* transposon. Meanwhile, $bla_{CTX\text{-}M\text{-}14}$, $bla_{CTX\text{-}M\text{-}27}$, and $bla_{CTX\text{-}M\text{-}65}$ show a distinct evolutionary relationship with other CTX-M variants through shared mobile genetic elements, particularly IS26, suggesting a potential coevolutionary origin.

3.2. Biogeographic Implications of *Escherichia coli* CTX-M Based on Haplotype Network

The haplotype map enabled investigation of *bla*CTX-M gene variants at the population level and examination of the origins of certain disease (49). Based on DnaSP analysis, the *E. coli* D4DU2 CTX-M sample, along with the other *E. coli* CTX-M group samples, has a high haplotype diversity (Hd) value of 0,9444. The haplotype network revealed seven distinct haplotypes (H1–H7), diverging from the major haplotype group H_7, which likely represents the ancestral or globally dominant form of CTX-M β-lactamase genes. Notably, D4DU2-ESBL-EC, represented by H_2, was connected to CTX-M-123 (H_7) via multiple median vectors (mv1 and mv4), indicating several unique mutational events and possibly missing evolutionary links.

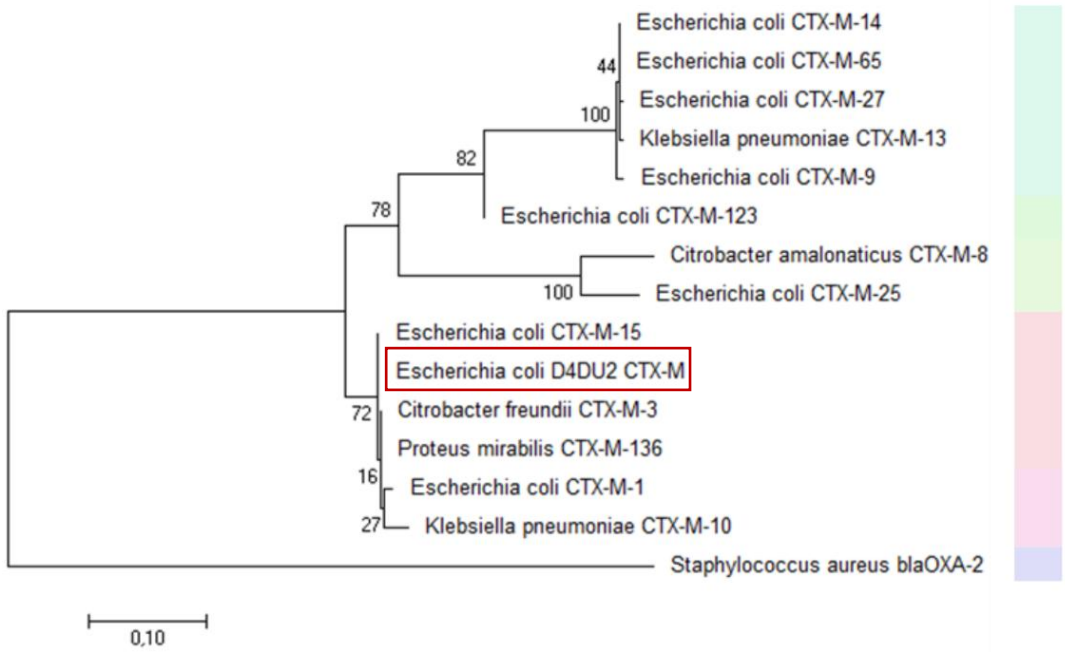

Figure 1. Evolutionary relationship of D4DU2-ESBL-EC with CTX-M variant based on a phylogenetic tree constructed with the ML method using MEGA7 with 1,000 bootstrap values

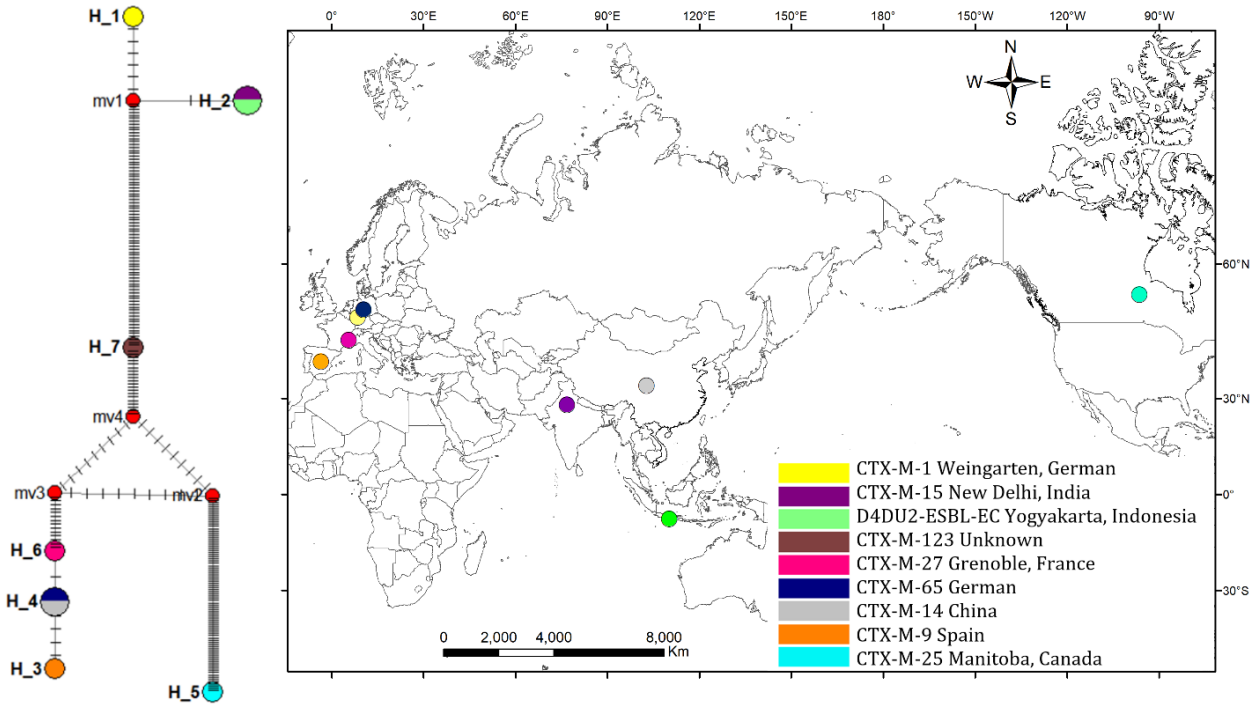

Figure 2. Haplotype map of *E. coli* CTX-M biogeographical distribution based on Network 10.2.0.0 analysis

The haplotype result (Figure 2) was fairly representative and correlated with the phylogenetic tree result. From the haplotype map, it can be found that the first case of *E. coli* CTX-M-1 was reported in Weingarten, Germany, in 1989 from an isolate clinically resistant to cefotaxime (50). The *E. coli* CTX-M-1 with haplotype 1 then dispersed to another country, where it mutated into haplotype 2 (CTX-M-15 and *E. coli* D4DU2 CTX-M) and haplotype 7 (CTX-M-123), which still retained the same serine-utilizing hydrolase sequence pattern. The serine-utilizing-hydrolases sequence encodes the penicillin-binding transpeptidase enzyme, so it will be inherited from the ancestor to the next generation (51). The gene that is inherited from the same parent will be shown as a haplotype (52).

Isolate which carried out haplotype 7 (CTX-M-123), then dispersed to another country and developed into haplotype 6 (CTX-M-27) and haplotype 5 (CTX-M-25), which contain different patterns of enzyme. Isolate *E. coli* CTX-M-25, which carried out haplotype 5 in Manitoba, Canada, has higher genetic variation than other isolates. The evolution of the CTX-M variant may have occurred due to continuous exposure of the isolate to various types of antibiotics, which exert selective pressure and promote the accumulation of adaptive mutations (53). Genetic resistance, co-transfer, and mutation may occur among bacterial genera that infect humans or animals. Random use of antibiotics in public or poultry farms without restrictive regulation will increase the mutation rate (54).

In addition, haplotype 6 (CTX-M-27), which originally emerged in France, appears to have diverged through sequential mutations. It first gave rise to two haplotype 4 (CTX-M-65 in Germany and CTX-M-14 in China) and subsequently to haplotype 3 (CTX-M-9 in Spain). This indicates a mutation sequence in which haplotype 6 is ancestral to both haplotype 4 and haplotype 3. The shared haplotype between isolates from Germany and China suggests the spread of the same *E. coli* CTX-M variant in both countries, usually through human mobility or the food chain (55). This geographical distribution of haplotype suggests the possibility of independent adaptive evolution of CTX-M variants, shaped by local selective pressures and antibiotic use patterns.

3.3. Pairwise Genetic Distance Analysis of *Escherichia coli* CTX-M

Pairwise distance showed relationships among ESBL isolates, with the least single-nucleotide polymorphism differences, highlighting the potential for close genetic relatedness and transmission of CTX-M-producing strains (48). The number of pairwise distances (Table 1) shows that *E. coli* CTX-M-14 (China) has consecutive values similar to those of CTX-M-65 (Germany), starting with 0,178, then 0,006, etc. This confirms that CTX-M-14 and 65 are the same *E. coli* isolates that migrate to different regions, as indicated by the similarity of haplotype 4 and the lowest genetic distance of 0.000 to other isolates. The pairwise genetic distance results also support the haplotype map, as both isolates are closely related to CTX-M-9 (Spain) and CTX-M-27 (France), with a genetic distance of 0.006.

Meanwhile, other isolates sharing the same haplotype, such as *E. coli* D4DU2, show a pairwise genetic distance of 0.012 from CTX-M-15. In *E. coli* CTX-M-15, the corresponding value was 0.018, while in *E. coli* D4DU2 it was 0.030. Both values were lower than the CTX-M-1. Additionally, compared to other CTX-M types, D4DU2 exhibits genetic distances

ranging from 0.111 (with CTX-M-123) to 0.192 (with CTX-M-9), suggesting significant nucleotide variation (56). The results indicate that *E. coli* D4DU2 represents a potential novel variant of the *bla*CTX-M gene, distinct from *E. coli* CTX-M-15, even though both share the same serine-utilizing-hydrolases sequence (haplotype 2).

3.4. Amino Acid Substitution and Characterization of *Escherichia coli* CTX-M Variants

The amino acid analysis (Table 2) shows that some *E. coli* CTX-M groups share the same haplotype. For example, *E. coli* CTX-M-14 from China and CTX-M-65 from Germany (H4) differ in the groups CTX-M-14 and CTX-M-65, which occur at positions V80A and S275R, respectively. The *E. coli* D4DU2-ESBL-EC Isolate from Demangan Traditional Market, Indonesia, shares haplotype H2 and the serine-utilizing-hydrolases sequence with CTX-M-15 from New Delhi, India. However, *E. coli* D4DU2-ESBL-EC harbors unique mutations at W253L and P254A, distinguishing it from CTX-M-15. Other isolates exhibited characteristic polymorphisms that matched their respective CTX-M groups. For instance, CTX-M-9, CTX-M-14, CTX-M-27, and CTX-M-65 share substitutions at positions 80 (Alanine) and 86 (Cystein), indicating a close genetic relationship within this clade.

Comparative amino acid sequence analysis of the CTX-M β-lactamase family identified multiple conserved and polymorphic sites among the studied isolates (Table 2). CTX-M-123 represents a distinct haplotype, but amino acid alignment shows it has high sequence similarity to CTX-M-15 and D4DU2-ESBL-EC. D4DU2 differs from both CTX-M-15 and CTX-M-123 by unique mutations at amino acid positions 80, 253, 254, and 275. At position 80, most CTX-M variants carry valine (CTX-M-1/25/65) or alanine (CTX-M-9/14/15/27/123), but D4DU2 lacks this residue. At position 253, all CTX-M variants contain tryptophan, while D4DU2 has leucine. Similarly, at position 254, D4DU2 substitutes proline with alanine. At position 275, serine is present in all CTX-M variants except CTX-M-65 (arginine) and D4DU2 (deletion). These substitutions define polymorphic sites, demonstrating the novelty of D4DU2 as a CTX-M variant. Further investigations are required to determine how these amino acid changes affect β-lactamase function and bacterial resistance (57).

Table 1. Pairwise distance of *E. coli* CTX-M

Isolate	1	2	3	4	5	6	7	8	9
E. coli CTX-M-1		0,034	0,033	0,010	0,035	0,034	0,033	0,028	0,012
E. coli CTX-M-9	0,185		0,005	0,033	0,030	0,007	0,005	0,020	0,034
E. coli CTX-M-14	0,178	0,006		0,032	0,030	0,005	0,000	0,019	0,033
E. coli CTX-M-15	0,018	0,178	0,171		0,033	0,031	0,032	0,025	0,008
E. coli CTX-M-25	0,192	0,144	0,137	0,171		0,029	0,030	0,032	0,034
E. coli CTX-M-27	0,185	0,012	0,006	0,164	0,130		0,005	0,018	0,033
E. coli CTX-M-65	0,178	0,006	0,000	0,171	0,137	0,006		0,019	0,033
E. coli CTX-M-123	0,117	0,072	0,066	0,098	0,157	0,060	0,066		0,025
E. coli D4DU2	0,030	0,192	0,185	0,012	0,185	0,178	0,185	0,111	

1: *E. coli* CTX-M-1, 2: *E. coli* CTX-M-9, 3: *E. coli* CTX-M-14, 4: *E. coli* CTX-M-15, 5: *E. coli* CTX-M-25, 6: *E. coli* CTX-M-27, 7: *E. coli* CTX-M-65, 8: *E. coli* CTX-M-123, 9: *E. coli* D4DU2. The blue color represents low variability, as indicated by the standard deviation in MEGA7, which ranges from 0.000 to 0.035, suggesting that the distance between genetic pairs is highly consistent.

Table 2. Amino acid sequence comparison of *E. coli* D4DU2 with CTX-M variants

Source	Isolate	H	Serine-utilising Hydrolases	Polymorphic site												
				80	86	95	97	106	117	136	143	234	242	253	254	275
NG_048897.1	*E. coli* CTX-M-1	H1	SESEPNLLNQRVEIK	V	K	N	R	V	D	V	S	V	D	W	P	S
NG_049043.1	*E. coli* CTX-M-9	H3	SETQKQLLNQPVEIK	A	C	.	P	.	N	T	A	A	.	.	.	.
NG_048929.1	*E. coli* CTX-M-14	H4	SETQKQLLNQPVEIK	A	C	.	P	.	N	T	A	.	.	.	.	.
NG_048935.1	*E. coli* CTX-M-15	H2	SESEPNLLNQRVEIK	A	.	.	.	.	N	.	A	.	G	.	.	.
NG_048974.1	*E. coli* CTX-M-25	H5	SETQKGLLSQRVEIK	.	C	S	.	I	N	T	A	.	G	.	.	.
NG_048976.1	*E. coli* CTX-M-27	H6	SETQKQLLNQPVEIK	A	C	.	P	.	N	T	A	.	G	.	.	.
NG_049016.1	*E. coli* CTX-M-65	H4	SETQKQLLNQPVEIK	.	C	.	P	.	N	T	A	.	.	.	.	R
NG_048916.1	*E. coli* CTX-M-123	H7	SESEPNLLNQRVEIK	A	.	.	.	.	N	T	A	.	G	.	.	.
D4DU2-ESBL	*E. coli* D4DU2	H2	SESEPNLLNQRVEIK	-	.	.	.	.	N	.	A	.	G	L	A	-

H : haplotype, V: valine, K: Lysine, N: Asparagine, R: Arginine, I: Isoleucine, D: Aspartic acid, T: Threonine, A: Alanine, G: Glycine, W: trypthophan, E: Glutamic acid, S: Serine, Q: Glutamine, C: Cystein, P: Proline, L: Leucine

3.5. Structural Modeling of CTX-M Enzyme Using I-TASSER and SWISS-MODEL

Although the D4DU2-ESBL EC from the food source sample (Figure 3A and 3B) shows features of a β-lactamase, this protein differs from the reference protein found in clinical samples, *E. coli* CTX-M-15 (PDB ID: 7TI0 (Figure 3C). The W253L and P254A changes in D4DU2-ESBL-EC modify its shape: the β-sheet is more compact, and the α-helix is shorter than in the reference. 3D models show differences in the number of β-sheets. I-TASSER predicts two β-sheets for D4DU2-ESBL-EC. SWISS-ADME predicts three. CTX-M-15 has four β-sheets, each with a related domain. In CTX-M, β-sheets are key to enzyme activity and influence folding and stability in class A β-lactamases (58).

3.6. Comparative Validation of The Predicted CTX-M Structural Models

MolProbity validation showed that the 3D β-lactamase structure in D4DU2-ESBL-EC predicted by I-TASSER had a lower Ramachandran favored value of 86.80% and a non-ideal Rama z-score (-3.16) (Table 3). In contrast, SWISS-MODEL prediction demonstrated greater reliability and superior stereochemical quality across most MolProbity parameters, consistent with previous studies (59). The high-quality 3D structure of the β-lactamase enzyme in D4DU2-ESBL-EC, as assessed by SWISS-ADME, showed a Ramachandran plot of 97.44% and a MolProbity score at the 100th percentile. However, validation also showed the superiority of I-TASSER in visualizing protein 3D structures through predictions from amino acid sequences (60). Further validation with SAVES v6.1 showed that I-TASSER had better 3D proportion and strong compatibility with a 3D verification value of 83.42% (PASS), compared to SWISS-MODEL, which showed a failed result (70.05%). Nonetheless, all Ramachandran plot criteria and ERRAT scores indicate that SWISS-MODEL is more physically realistic than I-TASSER, based on steric rotational stability of the protein backbone.

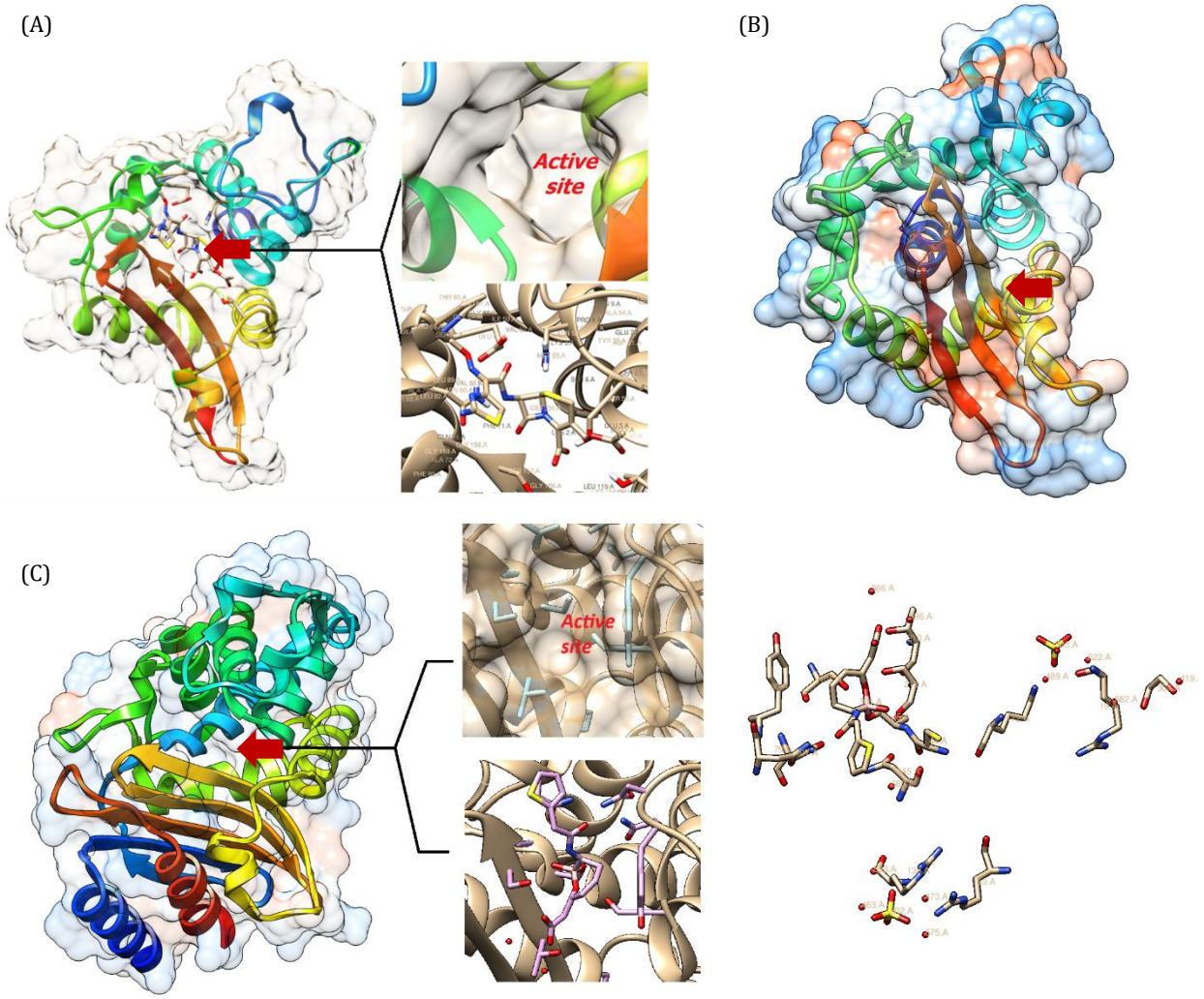

Figure 3. The 3D model of D4DU2 β-lactamase enzyme predicted by I-TASSER (A) and SWISS MODEL (B), compared to reference protein *E. coli* CTX-M-15 (PDB ID: 7TI0) from the PDB database (C), with red arrow showing the binding pocket of the active site.

Table 3. Comparative validation value of D4DU2-ESBL-EC protein prediction model using I-TASSER and SWISS-MODEL

Statistics Criteria	Validation Score of D4DU2-ESBL-EC Prediction		Good Validation Criteria
	I-TASSER	SWISS-MODEL	
MolProbity			
Clash score, all atom	98th percentile	99th percentile	Percentile ≥ 66
Ramachandran outliers	2.54%	0.51%	Outliers ≤ 0.05%
Ramachandran favored	86.80%	97.44%	Favored ≥ 98%
Rama distribution Z-score	-3.16 ± 0.51	1.67 ± 0.61	Abs(Z-score) ≤ 2
MolProbity score	48th percentile	100th percentile	Percentile ≥ 66
Bad bonds	0.00%	0.07%	Outlier bonds < 0.01%
CaBLAM outliers	2.6%	0.0%	Outliers ≤ 1%
CA Geometry outliers	0.51%	0.00%	Outliers ≤ 0.5%
SAVESv6.1			
All Ramachandrans	ERROR	PASS	PASS
Chi1-Chi2 plots	PASS	PASS	PASS
Ramachandran Plot-Favored Region	78.4%	92.3%	≥ 90%
Ramachandran Plot-Allowed Region	20.5%	7.1%	-
Errat	96.858	98.941	≥ 95%
Verify 3D	83.42% (PASS)	70.05% (FAILED)	≥ 80%

A Ramachandran plot (Figure 3C and 3D) was generated using SAVESv6.1 to evaluate the stereochemical quality of the predicted three-dimensional (3D) structure of the *Escherichia coli* D4DU2 CTX-M protein model (Figure 4). This plot maps the dihedral angles phi (ϕ) and psi (ψ) of the amino acid residues, allowing assessment of backbone conformational preferences and identifying residues in energetically favorable regions (61). In the *E. coli* D4DU2 CTX-M protein model using I-TASSER, 78.4% (134 out of 171) of the ASN48, ALA153, and PRO101 residues were found to occupy the most favored regions of the Ramachandran plot (A, B, and L regions). Meanwhile, the *E. coli* D4DU2 CTX-M protein model prediction using SWISS-MODEL has 92.3% (156 out of 197) in the Ramachandran favored region. Additionally, only one end residue (excluding Gly and Pro) was observed in the SWISS-MODEL Ramachandran plot, highlighting the completeness and integrity of the structure. Protein 3D structure prediction using I-TASSER and SWISS-MODEL showed that 20.5% (35 residues) and 7.1% (12 residues) were located in the additionally allowed regions (a, b, l, and p regions), and no residues were found in the generously allowed regionsPredictions using I-TASSER resulted in 2 residues (1.2%) in the disallowed region, whereas SWISS-MODEL resulted in only 1 residue (0.6%), indicating minimal deviation from the ideal geometry.

The Ramachandran analysis using both MolProbity and SAVESv6.1 demonstrates that the predicted protein models from I-TASSER and SWISS-MODEL exhibit good stereochemical quality. According to the criteria for a well-refined model (≥2.0 Å resolution and R-factor <20%), a model is expected to have over 90% of residues in the most favored regions (61). Only minor deviations showed in the current model, which are unlikely to significantly impact the structural integrity. Side-chain torsional strain, chirality, backbone torsion angles, and local geometric quality across the protein sequence (62) were analyzed via PROCHECK (Figure 5). Overall side-chain geometry showed good results, with most residues remaining within acceptable deviation limits and being stereochemically valid. Based on the predicted secondary structure, the D4DU2-ESBL-EC enzyme element consists of a folded and globular protein with the majority located in the most favorable (green triangles) or allowed (blue squares) regions (63). Only a few residues have zeta torsion deviations greater than 2.0. This is also supported by the G-factor scores, which indicate all structures are within the acceptable range (yellow to orange), although some red residues indicate an unfavorable region.

Amino acids substitution into Leucine at position 253 and Alanine at position 254 can also be observed in the Ramachandran plot, which shows that the number of Alanine (Ala, 25 residues) is the most abundant compared to other amino acids, followed by Leucine (Leu, 19 residues). Most Ala and Leu are found in the favorable region of the D4DU2-ESBL-EC protein. The plot also shows that of 13 Serine (Ser) residues, 10 are sterically favorable. Serine plays a crucial role in forming the conserved serine hydrolase domain in the β-lactamase enzyme. Based on two side-chain torsion angles (Chi1 and Chi2) analysis with PROCHECK, the D4DU2-ESBL-EC CTX-M protein model predicted by I-TASSER maintains the appropriate side-chain geometry and is consistent with the well-defined experimental structure. The largest number of residues in the structural model of the D4DU2-ESBL-EC CTX-M protein predicted by I-TASSER is Leucine, with 20 residues, of which 4 are rotamer outliers and 16 show stable, realistic Leu side-chain conformations. This is in accordance with the results of the 253 amino acid substitution, which indicate leucine at that position. Meanwhile, both Lysine (Lys) and Asparagine (Asn) have 11 residues, with 7 rotamer outliers. Meanwhile, no Cysteine (Cys) residues were found in sufficient quantity to be plotted. Residues such as Phenylalanine (Phe, 3 residues), methionine (Met, 5 residues), and Tyrosine (Tyr, 4 residues) predominantly occupy the high-resolution zone (≤2.0Å) in the green shaded region, indicating that the modeled structure largely adopts sterically and energetically more favorable conformations. However, amino acids such as Histidine (His, 3 residues), Tryptophan (Trp, 3 residues), and Aspartic Acid (Asp, 10 residues) exhibit potential local strain or flexibility in less favorable regions.

3.7. Functional Analysis of D4DU2-ESBL-EC Active Site Mutations

A two-way analysis of variance (ANOVA) indicated that protein type (D4DU2, 1IYP, and 3BFC) significantly influenced the binding affinity to β-lactam antibiotics (including cephalosporins and penicillin derivatives). This conclusion is supported by the F statistic ($F(2,34) = 24.545$, $p < 0.001$), which indicates a low probability that the result occurred by chance. However, Levene's test revealed a violation of homogeneity ($p = 0.002$), suggesting unequal variance among groups. Nonetheless, because the sample sizes were equal across groups (balanced design), the ANOVA was considered sufficiently robust, which permitted interpretation of the results (64).

The docking results show a moderate binding affinity of -5.3 to -7.3 kcal/mol; this value is often reported for interactions between β-lactam antibiotics and β-lactamase enzymes such as CTX-M-15 (65). D4DU2-ESBL-EC showed the weakest mean affinity (-6.11 kcal/mol), while wild-type proteins 1IYP and 3BFC had -6.44 and -6.68 kcal/mol, respectively. The predicted mutant D4DU2 variant's higher affinity score suggests that structural changes reduce the ability of antibiotics such as Cephalosporins (-6.43 kcal/mol) or inhibitors such as Avibactam (-5.83 kcal/mol) to stably occupy the active site. In contrast, Cephalosporins bind more stably in the wild-type CTX-M-15 protein 3BFC (-7.33 kcal/mol) and also in 1IYP (-7.17 kcal/mol). For Urobactam, 3BFC showed a lower binding affinity (-7.23 kcal/mol) than the other proteins.

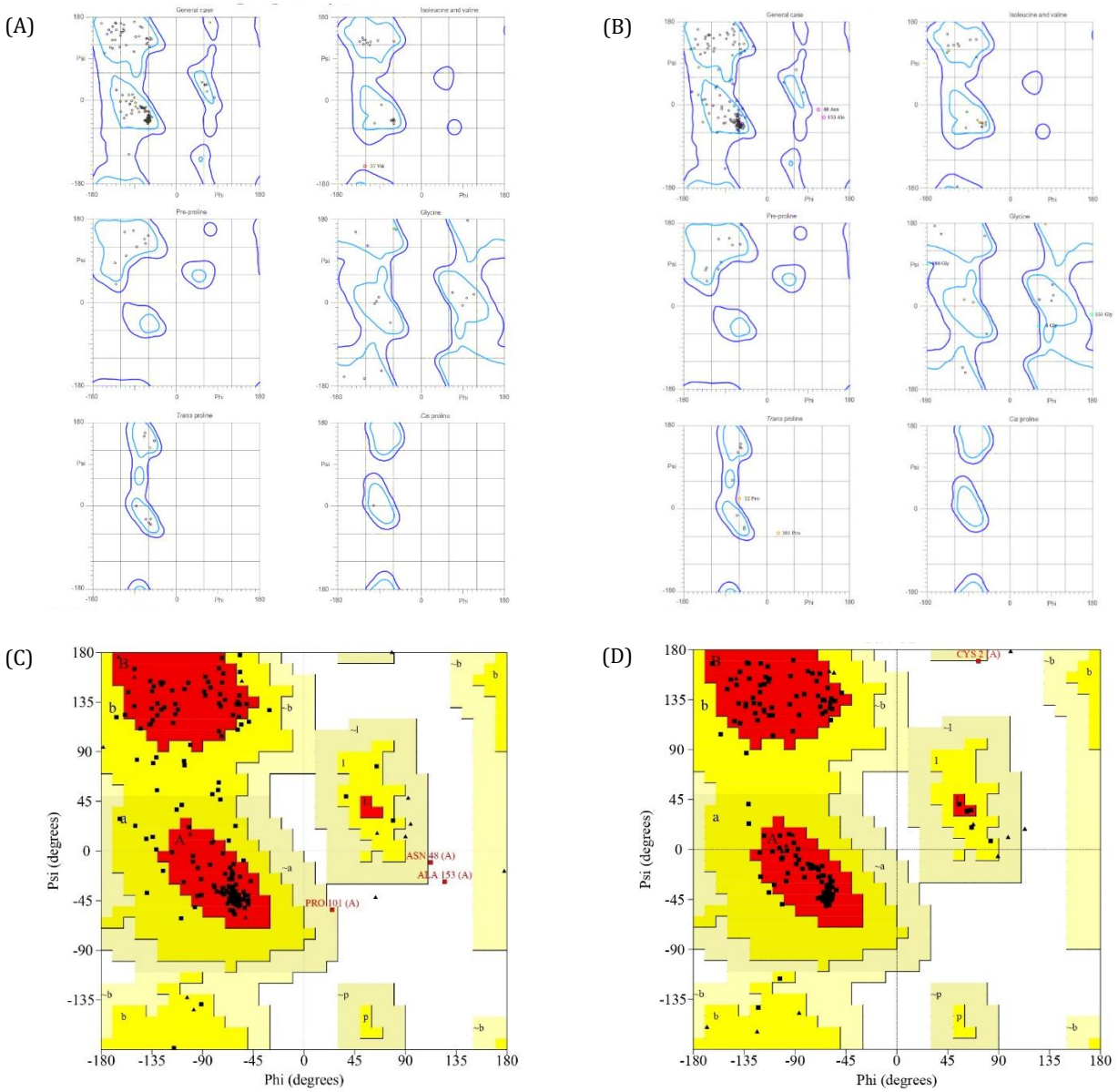

Figure 4. Ramachandran plot of the predicted 3D structure of *E. coli* D4DU2 CTX-M protein model using I-TASSER (A) and SWISS-MODEL (B) validated by MolProbity, and Ramachandran plot of the predicted 3D structure of *E. coli* D4DU2 CTX-M protein model using I-TASSER (C) and SWISS-MODEL (D) validated by SAVESv6.1

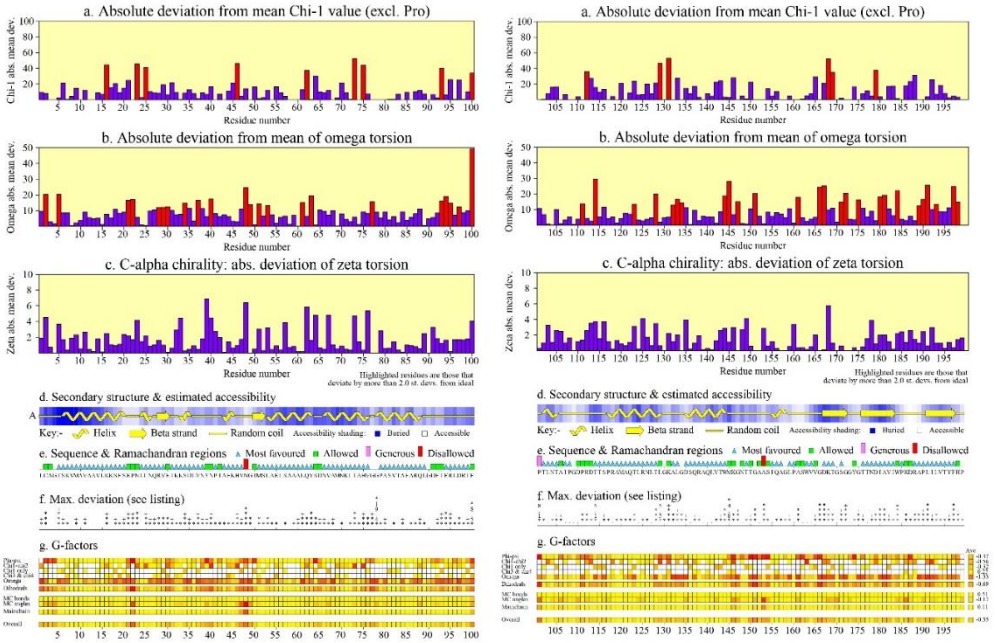

Figure 5. Residue properties of D4DU2-ESBL-EC protein predicted by I-TASSER based on analysis via PROCHECK

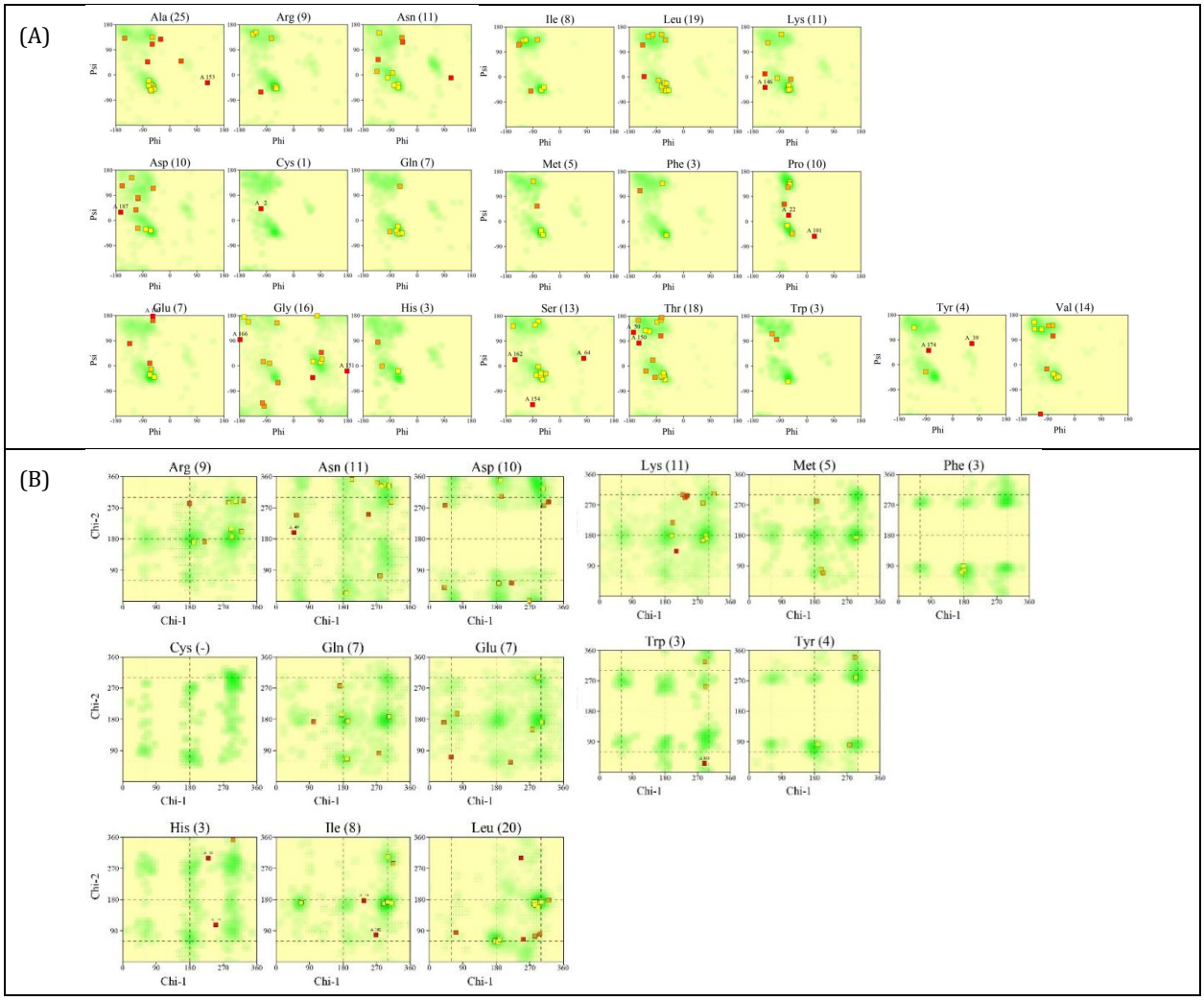

Figure 6. The quality of the chain conformations of the structural model of the D4DU2-ESBL-EC CTX-M protein predicted by I-TASSER based on (A) Ramachandran plots and (B) Chi1-Chi2 plots. Parentheses indicate the number of residues in the structure. Yellow squares represent residues located in the shaded green favorable conformational region with high-resolution (≤ 2.0 Å). Red squares or triangles indicate residues in unfavorable regions (scores <-3.0Å)

In the native 1IYP and 3BFC proteins, Ser130, Asn104, Asn132, and Thr235 catalyze hydrolysis of the β-lactam ring by stabilizing enzyme-substrate interactions in the class A β-lactamase active site (65). In contrast, the predicted D4DU-ESBL-EC variant exhibits a shift in the orientation of the binding pocket and loses the canonical Ser residue, replacing it with a hydrogen bond involving Cys2, Leu1, Asp110, and Thr115. These changes suggest that substitutions at W253L and P254A, both near the catalytic region, cause structural rearrangements. These mutations may alter local folding and the positions of side chains that define the pocket geometry (66), thereby reducing the stability of β-lactam antibiotic binding (67). Antibiotics, therefore, bind less strongly to D4DU2-ESBL-EC, reducing inhibition and increasing resistance in the new CTX-M variant. However, the binding differences are small (0.3-0.9 kcal/mol), so this only provides a preliminary indication.

This study offers a novel contribution to the understanding of the new mutant variant of extended-spectrum β-lactamase (ESBL)-producing *E. coli* originating from food sources in Indonesia. In contrast to previous studies that largely focused on CTX-M variants originating from hospitals (13,15), our study highlights the growing concern about antimicrobial resistance (AMR) within the One Health framework in the food chain. Especially because of mutations at amino acid positions W253L and P254A, which affect conformational flexibility and the antibiotic spectrum (68). Overall, this study combines genomic, structural, and computational approaches to provide new insights into the molecular features and inhibitory potential of food-derived CTX-M enzymes.

Table 4. Molecular docking of β-lactam antibiotics on several CTX-M proteins with different binding affinities variation

Antibiotic	Binding Affinity (Kcal/Mol) with Protein			
	Code: D4DU2	PDB ID: 1IYP	PDB ID: 3BFC	x̄ for Antibiotics
Urobactam	-6.433 ± 0.233	-6.300 ± 0.115	-7.233 ± 0.033	-6.656^{cd}
Penicillin	-6.467 ± 0.133	-6.167 ± 0.133	-6.600 ± 0.300	-6.411^{bc}
Cephalosporin	-6.433 ± 0.067	-7.167 ± 0.088	-7.333 ± 0.067	-6.978^{e}
(5R)-Carbapenem	-5.367 ± 0.145	-5.867 ± 0.033	-5.833 ± 0.067	-5.688^{a}
Avibactam	-5.833 ± 0.176	-6.333 ± 0.145	-6.767 ± 0.233	-6.311^{b}
Native Ligand				
Cephalothin		-6.833 ± 0.145		-6.833^{de}
Imipenem			-6.333 ± 0.033	-6.333^{b}
x̄ for Protein	6.107^{a}	6.444^{b}	6.683^{c}	

x̄ : mean value; the number following ± indicates the standard error; ^{a,b,c,d,e} : subsets identified by Duncan's post hoc test ($p<0.05$) conducted with significance level of α =0.05 and mean square (Error) = 0.065

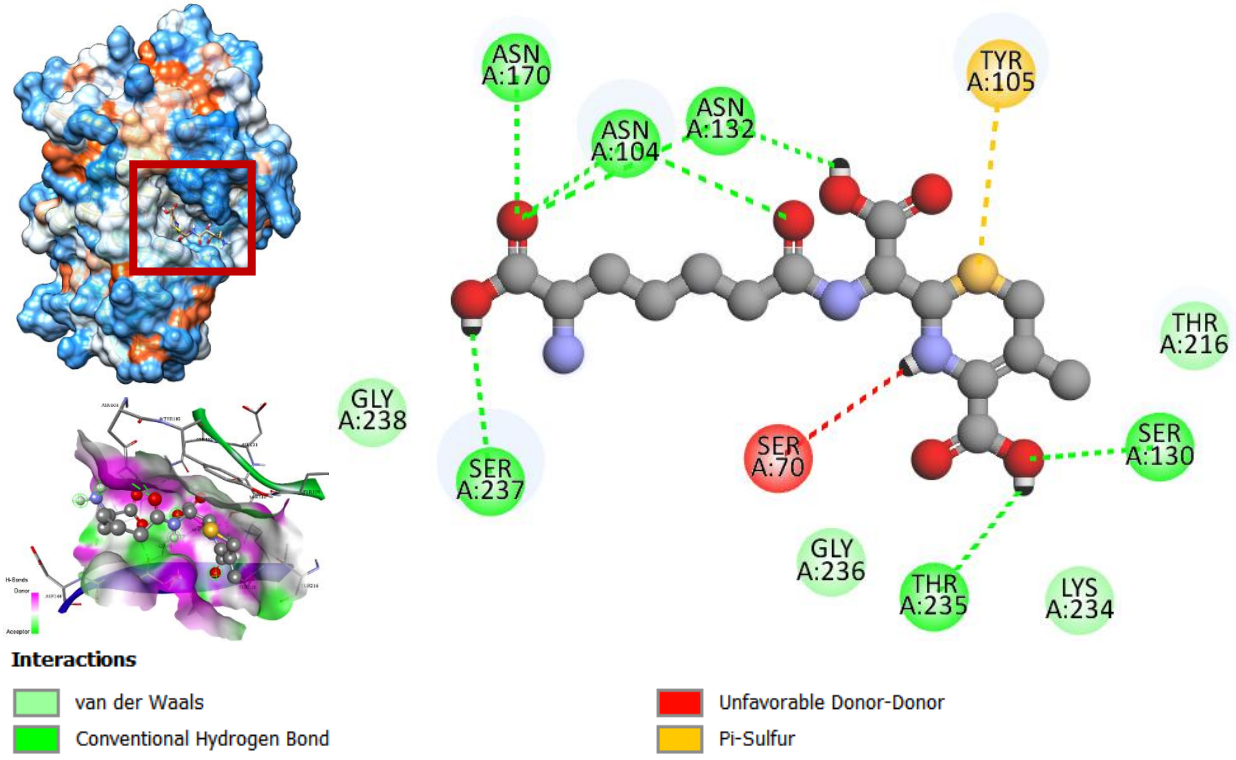

Figure 7. Interaction of the ligand binding pocket of the β-lactamase protein Toho-1 (PDB ID: 1IYP) derived from Escherichia coli with Cephalosporins. Blue region indicates hydrophilic (polar) areas, red regions represent hydrophobic (nonpolar) areas, green region typically represents the hydrogen-bond acceptor, and pink (magenta) region represents the hydrogen-bond donor. ASN: Asparagine, TYR: Tyrosine, THR: Threonine, SER: Serine, LYS: Lysine, GLY: Glycine.

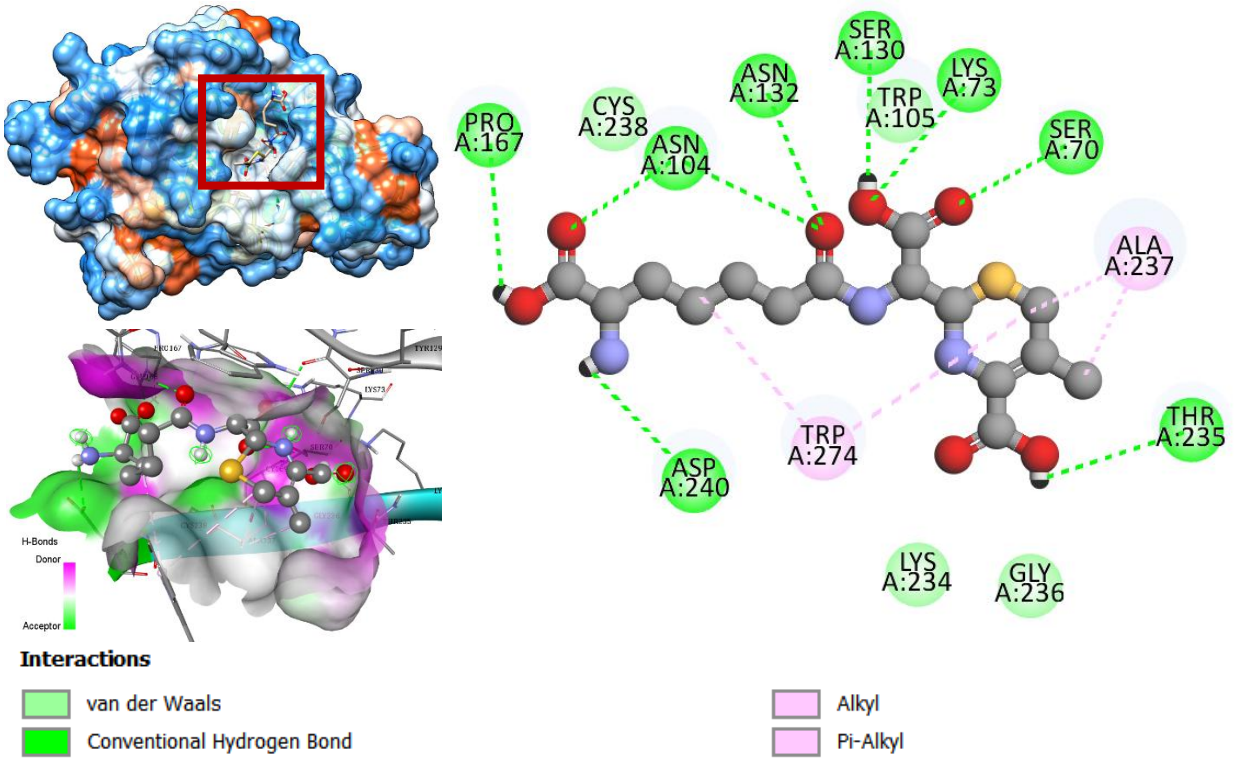

Figure 8. Ligand binding pocket interaction of the class A β-lactamase protein (PDB ID: 3BCF) isolated from *E. coli* BL21 with Cephalosporin. Blue region indicates hydrophilic (polar) areas, red regions represent hydrophobic (nonpolar) areas, green region typically represents the hydrogen-bond acceptor, and pink (magenta) regions represent the hydrogen-bond donor. PRO: Proline, CYS: Cysteine, ASN: Asparagine, SER: Serine, TRP: Tryptophan, LYS: Lysine, ALA: Alanine, THR: Threonine, GLY: Glycine, ASP: Aspartic Acid

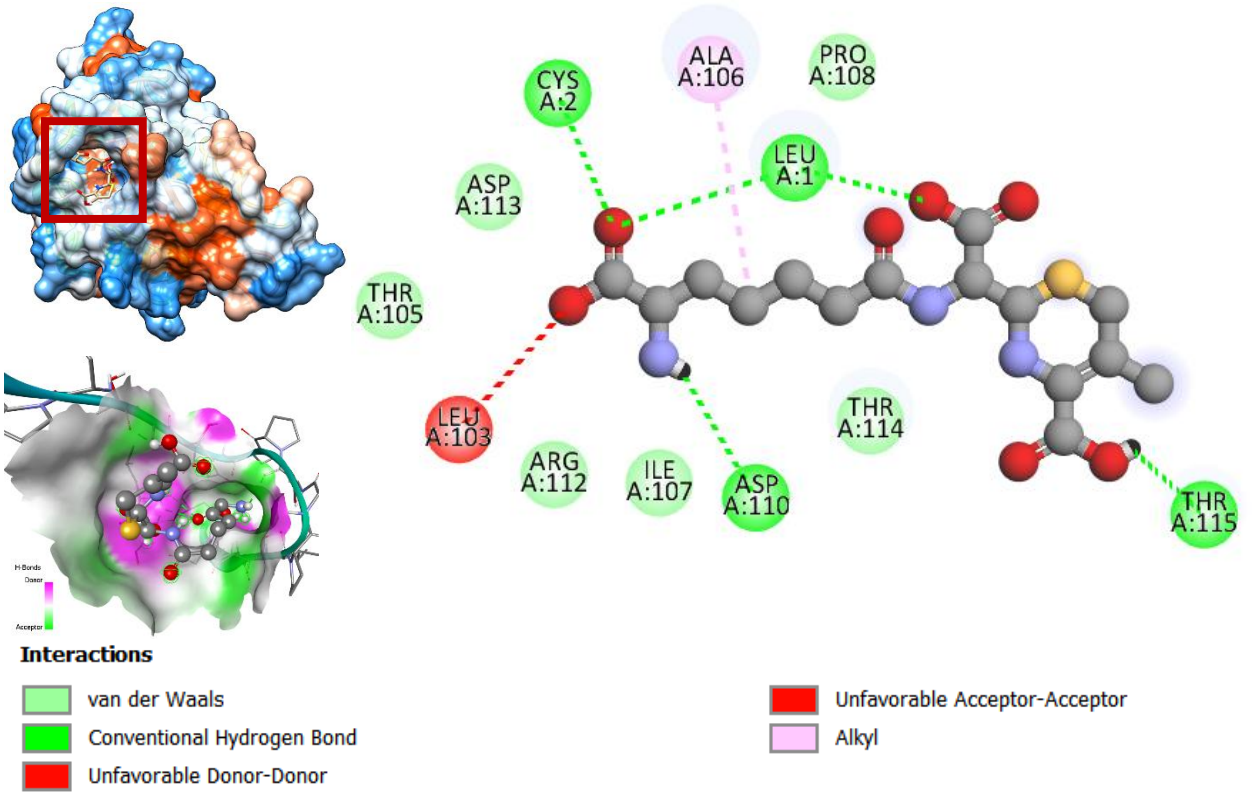

Figure 9. Ligand binding pocket interaction of the D4DU2-ESBL-EC with Cephalosporin. Blue region indicates hydrophilic (polar) areas, red regions represent hydrophobic (nonpolar) areas, green region typically represents the hydrogen-bond acceptor, and pink (magenta) represents the hydrogen bond donor. ILE: Isoleucine, LEU: Leucine, ARG: Arginine

This study provides valuable insights, but several limitations remain. First, while in silico approaches generate hypotheses, they cannot replace experimental validation. Therefore, it is necessary to confirm the inhibitory activity of tested antibiotics against CTX-M enzymes using in vitro enzymatic assays or in vivo antimicrobial susceptibility testing (69). Second, the docking analysis used static conditions and may therefore not capture the full dynamics of protein-ligand interactions. To address this, molecular dynamics (MD) simulations should be included for a clearer picture of binding stability and conformational changes over time (70). Third, the study evaluated a relatively narrow range of antibiotics, specifically beta-lactams. Additionally, only one structural model (*E. coli* D4DU2 CTX-M) and three reference proteins were used for comparison, which may not fully reflect the structural diversity of CTX-M enzymes across various bacterial strains. Taken together, these considerations highlight those future studies should integrate experimental validation and advanced simulations to support and expand on these findings.

4. CONCLUSIONS

Based on the result and discussion, *E. coli* (D4DU2-ESBL-EC) is a new variant from Yogyakarta, Indonesia, closely related to Indian blaCTX-M-15 variants. Point mutations in *E. coli* D4DU2, such as W253L, P254A, and the putative binding site, differentiate it from CTX-M-15. Stereochemical evaluation using MolProbity, SAVES, and PROCHECK shows that the predicted 3D CTX-M β-lactamase structure from *E. coli* Yogyakarta, generated by I-TASSER and SWISS-MODEL, is considered good. Although in the I-TASSER prediction, the percentage of residues in the most favored regions (78.4%) is slightly below the ideal benchmark (>90% for high-resolution structures), the model remains structurally sound and suitable for further computational analysis, such as molecular docking and dynamic simulations. Overall, this study demonstrates that I-TASSER, complemented by PROCHECK validation, offers a valuable in silico approach for the structural characterization of ESBL proteins from foodborne bacterial isolates in resource-limited contexts. However, SWISS-MODEL is recommended for 3D structure prediction.

Author contributions: AK: Methodology, Software, Validation, Formal analysis, Investigation, Writing original draft preparation, Visualization, Funding acquisition. ER: Resources, Data curation, Review and editing, Supervision. All authors have read and agreed to the published version of the manuscript.

Funding: This research received no external funding.

Acknowledgements: None.

Ethics statement: None.

Conflict of interest: None.

REFERENCES

1. Bonten M, Johnson JR, Biggelaar AHJ, Georgalis L., Geurtsen J, de Palacios PI, Gravenstein S, Verstraeten T, Hermans P, Poolman JT. Epidemiology of *Escherichia coli* bacteremia: A systematic literature review. Clin Infect Dis. 2021;72(7):1211-1219. https://doi.org/10.1093/cid/ciaa210
2. Golden CE, Rothrock MJ Jr, Mishra A. Mapping foodborne pathogen contamination throughout the conventional and alternative poultry supply chains. Poult Sci. 2021;100(7):101157 https://doi.org/10.1016/j.psj.2021.101157
3. Wilcox CH, Sandilands V, Mayasari N, Asmara IY, Anang A. A literature review of broiler chicken welfare, husbandry, and assessment. World's Poult Sci J. 2023; 80(1):3–32. https://doi.org/10.1080/00439339.2023.2264824
4. Leahy E, Mutua F, Grace D, Lambertini E, Thomas LF. Foodborne zoonoses control in low-and middle-income countries: Identifying aspects of interventions relevant to traditional markets which act as hurdles when mitigating disease transmission. Front Sustain Food Syst. 2022;6:913560. https://doi.org/10.3389/fsufs.2022.913560
5. Kuan NL, Chen YP, Shien JH, Yeh KS. Characteristics of the extended spectrum-β-lactamase-producing *Escherichia coli* isolated from diseased livestock and poultry in Taiwan. Sci Rep. 2024;14(1):29459. https://doi.org/10.1038/s41598-024-80943-9
6. Lin X, and Kuck U. Cephalosporins as key lead generation beta-lactam antibiotics. Appl Microbiol Biotechnol. 2022;106(24):8007-8020. https://doi.org/10.1007/s00253-022-12272-8
7. Sudarwanto MB, Lukman DW, Latif H, Pisestyani H, Sukmawinata E, Akineden O, Usleber E. CTX-M Producing *Escherichia coli* isolated from cattle feces in Bogor slaughterhouse, Indonesia. Asi Pac J Tropic Biomedicine. 2016;6(7):605-608. https://doi.org/10.1016/j.apjtb.2016.05.001
8. Saliu EM, Vahjen W, Zentek J. Types and prevalence of extended-spectrum beta-lactamase producing Enterobacteriaceae in poultry. Anim Health Res Rev. 2017;18(1):46-57. https://doi.org/10.1017/s1466252317000020
9. Xu H, Tan C, Li C, Li J, Han Y, Tang Y, Lei C, Wang H. ESBL-*Escherichia coli* extracellular vesicles mediate bacterial resistance to β-lactam and mediate horizontal transfer of $bla_{CTX-M-55}$. Int J Antimicrob Agents. 2024;63(5):107145. https://doi.org/10.1016/j.ijantimicag.2024.107145

10. Handayani KS, Setiyono A, Lukman DW, Pisestyani H, Rahayu P. Distribution of extended-spectrum β-lactamase producing *Escherichia coli* genes in an integrated poultry-fish farming system in Bogor, Indonesia. Vet World. 2024;17(7):1596-1602. https://doi.org/10.14202/vetworld.2024.1596-1602

11. Ranjan A, Shaik S, Hussain A, Nandanwar N, Semmler TJadhav S, Wieler LH, Ahmed N. Genomic and functional portrait of a highly virulent, CTX-M-15-producing H30-Rx subclone of *Escherichia coli* sequence type 131. Antimicrob Agents Chemother. 2015; 59(10): 6087-6095. https://doi.org/10.1128/aac.01447-15

12. Ariyanti T, Noor SM, Rachmawati F, Widiyanti PM, Andriani, Sukmawinata E, Pisestyani H, Suhaemi, Mulyati S, Sukatma, Anastasia Y, Purba HHS. Prevalence, antibiotic resistance patterns, and genetic characterization of ESBL-producing *Escherichia coli* in chicken samples from Tangerang, Indonesia. IOP Conf. Series: Earth and Environmental Science. 2025;1471:1-6. https://doi.org/10.1088/1755-1315/1471/1/012062

13. Wardoyo EH, Sugawara Y, Nakano S, Zuo H, Elahi S, Arai C, Kondo K, Kuntaman K, Sugai M.0. Genomic characterization of extended-spectrum β-lactamase-producing *Escherichia coli* spread among chickens and healthy residents in Lombok, Indonesia. Appl Environ Microbiol. 2025;0:e02364-24. https://doi.org/10.1128/aem.02364-24

14. Aini Eka Puji Dameanti FN, Yanestria SM, Effendi MH, Plumeriastuti H, Tyasningsih W, Ugbo EN, Sutrisno R, Safri MAA. Genotyping of extended-spectrum beta-lactamase-producing *Escherichia coli* isolated from wastewater of dairy farms in East Java. Indonesia Vet World. 2025;18(1):162-171. https://doi.org/10.14202/vetworld.2025.162-171

15. Mardhia M, Liana DF, Mahyarudin M, Ih H. The first report of antibiotic resistance and virulence factor profiles in multidrug-resistant clinical isolates of Klebsiella pneumoniae from Pontianak, Indonesia. Osomh public health and research perspectives. 2025;16(2):160-168. https://doi.org/10.24171/j.phrp.2024.0242

16. Lengyel J, Hnath E, Storms M. Towards an integrative structural biology approach: combining Cryo-TEM, X-ray crystallography, and NMR. J Struct Funct Genomics, 2014;15: 117–124. https://doi.org/10.1007/s10969-014-9179-9

17. Papageorgiou AC, Poudel N, Mattsson J. Protein structure analysis and validation with X-ray crystallography. Protein downstream processing: design, development, and application of high and low-resolution methods. 2021;2178:377-404. https://doi.org/10.1007/978-1-0716-0775-6_25

18. Hu Y, Cheng K, He L, Zhang X, Jiang B, Jiang L, Li C, Wang G, Yang Y, Liu M. NMR-based methods for protein analysis. Anal Chem 2021;93:1866-1879. https://dx.doi.org/10.1021/acs.analchem.0c03830?ref=pdf

19. Chang WH, Huang SH, Lin HH, Chung SC, & Tu IP. Cryo-EM Analyses permit visualization of structural polymorphism of biological macromolecules. Frontiers in bioinformatics, 2021;1: 788308. https://doi.org/10.3389/fbinf.2021.788308

20. Chang WH, Huang SH, Lin HH, Chung SC, Tu IP. Cryo-EM Analyses permit visualization of structural polymorphism of biological macromolecules. Front Bioinform. 20218;1:788308. https://doi.org/10.1038/s41596-022-00728-0

21. Carugo O. Identifications of false positives amongst sodium(I) cations in protein three-dimensional structures—A validation approach extendible to any alkali or alkaline earth cation and to any monoatomic Anion. Crystals. 2024;14(11):918. https://doi.org/10.3390/cryst14110918

22. Rana C, Rajput S, Behera M, Gautam D, Vikas V, Vats A, Roshan M, Ghorai SM, De S. Global epidemiology of CTX-M-type β-lactam resistance in human and animal. Comp Immunol Microbiol Infect Dis. 2022;86:101815. https://doi.org/10.1016/j.cimid.2022.101815

23. Ghiglione B, Rodríguez MM, Brunetti F, Papp-Wallace KM, Yoshizumi A, Ishii Y, Bonomo RA, Gutkind G, Klinke S, Power P. Structural and biochemical characterization of the novel CTX-M-151 extended-spectrum β-Lactamase and its inhibition by avibactam. Antimicrob Agents Chemother. 2021;65(4):e01757-20. https://doi.org/10.1128/AAC.01757-20

24. Matesanz M, Mensa J. Ceftazidime-avibactam. Rev Esp Quimioter. 2021;34(Suppl1):38–40. https://doi.org/10.37201/req/s01.11.2021

25. Deshpande LM, Doyle TB, Sader HS, Castanheira M. Activity of aztreonam-avibactam and ceftazidime-avibactam against β-lactamase-producing enterobacterales Isolates from United States hospitals. J Glob Antimicrob Resist. 2025 Sep;44:103-110. https://doi.org/10.1016/j.jgar.2025.06.002

26. Rashid NNA, Nasir MHM, Hamzah N, Ismail CMKH, Hishamuddin SASN, Suffian IFM, Hamid AAA. Three-dimensional structure of human epididymis protein (HE4): A protein modelling of an ovarian cancer biomarker through in silico approach. J Trop Life Sci. 2024;14(2): 331-348. http://dx.doi.org/10.11594/jtls.14.02.13

27. Sayers EW, Beck J, Bolton EE, Brister JR, Chan J, Connor R, Feldgarden M, Fine AM, Funk K, Hoffman J, Kannan S, Kelly C, Klimke W, Kim S, Lathrop S, Marchler-Bauer A, Murphy TD, O'Sullivan C, Schmieder E, Skripchenko Y, Pruitt KD. Database resources of the National Center for Biotechnology Information in 2025. Nucleic Acids Res. 2025;53(D1):D20-D29. https://doi.org/10.1093/nar/gkae979

28. Reddy B, Fields R. Performance Analysis of Multiple Sequence Alignment Tools. In Proceedings of the 2024 ACM Southeast Conference (ACMSE '24). ACM. 2024:167–174. https://doi.org/10.1145/3603287.3651216

29. Tamura K, Stecher G, Kumar S. MEGA11: Molecular Evolutionary Genetics Analysis Version 11. Mol Biol Evol. 2021;38(7):3022-3027. https://doi.org/10.1093/molbev/msab120

30. Kumar S, Stecher G, Tamura K. MEGA7: Molecular Evolutionary Genetics Analysis Version 7.0 for Bigger Datasets. Mol Biol Evol. 2016;33(7):1870-1874. https://doi.org/10.1093/molbev/msw054

31. Rozas J, Ferrer-Mata A, Sánchez-DelBarrio JC, Guirao-Rico S, Librado P, Ramos-Onsins SE, Sánchez-Gracia A. DnaSP 6: DNA Sequence Polymorphism Analysis of Large Data Sets. Mol Biol Evol. 2017 Dec 1;34(12):3299-3302. https://doi.org/10.1093/molbev/msx248

32. Chi L, Dong Y, Wang R, Yang S, Wu L, Xue Y, Chen H. HapNetworkView: a tool for haplotype network exploration and visualization. BMC Genomics. 2025 Jan 20;26(1):52. https://doi.org/10.1186/s12864-025-11206-8

33. Waterhouse A, Bertoni M, Bienert S, Studer G, Tauriello G, Gumienny R, Heer FT, de Beer TAP, Rempfer C, Bordoli L, Lepore R, Schwede T. SWISS-MODEL: homology modelling of protein structures and complexes. Nucleic Acids Res. 2018;46(W1):W296-W303. https://doi.org/10.1093/nar/gky427

34. Zheng W, Zhang C, Li Y, Pearce R, Bell EW, Zhang Y. Folding non-homologous proteins by coupling deep-learning contact maps with I-TASSER assembly simulations. Cell Rep Methods. 2021;1(3):100014. https://doi.org/10.1016/j.crmeth.2021.100014

35. Yang J, Yan R, Roy A, Xu D, Poisson J, Zhang Y. The I-TASSER Suite: Protein structure and function prediction. Nat Methods. 2015;12(1):7-8. https://doi.org/10.1038/nmeth.3213

36. Galdino GT, DesCôteaux T, Teruel N, Najmanovich R. NRGSuite-Qt: a PyMOL plugin for high-throughput virtual screening, molecular docking, normal-mode analysis, the study of molecular interactions, and the detection of binding-site similarities. Bioinform Adv. 2025;5(1):vbaf129. https://doi.org/10.1093/bioadv/vbaf129

37. Biovia D, Berman H, Westbrook J, Feng Z, Gilliland G, Bhat T, Richmond TJTJoCP. Biovia Dassault System, Discovery Studio Visualizer, v21.1.0. San Diego. 2021;10:0021-9991

38. Laskowski RA, MacArthur MW, Mos DS, Thornton JM. PROCHECK a program to check the stereochemical quality of protein structures. J App Cryst. 1993;26:283-291. https://doi.org/10.1107/S0021889892009944

39. Williams CJ, Headd JJ, Moriarty NW, Prisant MG, Videau LL, Deis LN, Verma V, Keedy DA, Hintze BJ, Chen VB, Jain S, Lewis SM, Arendall WB, Snoeyink J, Adams PD, Lovell SC, Richardson JS, Richardson DC. MolProbity: More and better reference data for improved all-atom structure validation. Protein Sci. 2018;27(1):293-315. https://doi.org/10.1002/pro.3330

40. Kim S, Chen J, Cheng T, Gindulyte A, He J, He S, Li Q, Shoemaker BA, Thiessen PA, Yu B, Zaslavsky L, Zhang J, & Bolton EE. PubChem in 2021: new data content and improved web interfaces. Nucleic Acids Res. 2019;49: D1388–D1395. https://doi.org/10.1093/nar/gkaa971

41. Burley SK, Bhatt R, Bhikadiya C, Bi C, Biester A, Biswas P, Bittrich S, Blaumann S, Brown R, Chao H, Chithari VR, Craig PA, Crichlow GV, Duarte JM, Dutta S, Feng Z, Flatt JW, Ghosh S, Goodsell DS, Green RK, Guranovic V, Henry J, Hudson BP, Joy M, Kaelber JT, Khokhriakov I, Lai JS, Lawson CL, Liang Y, Myers-Turnbull D, Peisach E, Persikova I, Piehl DW, Pingale A, Rose Y, Sagendorf J, Sali A, Segura A, Sekharan M, Shao C, Smith J, Trumbull M, Vallat B, Voigt M, Webb B, Whetstone S, Wu-Wu A, Xing T, Young JY, Zalevsky A, Zardecki C, Updated resources for exploring experimentally-determined PDB structures and Computed Structure Models at the RCSB Protein Data Bank. Nucleic Acids Res, 2025;53(D1):D564–D574. https://doi.org/10.1093/nar/gkae1091

42. Pettersen EF, Goddard TD, Huang CC, Couch GS, Greenblatt DM, Meng EC, Ferrin TE. UCSF Chimera--a visualization system for exploratory research and analysis. J Comput Chem. 2004;25(13):1605-12. https://doi.org/10.1002/jcc.20084

43. Forli S, Huey R, Pique ME, Sanner MF, Goodsell DS, Olson AJ. Computational protein-ligand docking and virtual drug screening with the AutoDock suite. Nat Protoc. 2016;11(5):905-19. https://doi.org/10.1038/nprot.2016.051

44. Dallakyan S, Olson AJ. Small-molecule library screening by docking with PyRx. Methods Mol Biol. 2015;1263:243-50. https://doi.org/10.1007/978-1-4939-2269-7_19

45. Elmowalid GA, Ahmad AAM, Hassan MN, Abd El-Aziz NK, Abdelwahab AM, Elwan SI. Molecular detection of new SHV β-lactamase variants in clinical *Escherichia coli* and *Klebsiella pneumoniae* isolates from Egypt. Comp Immunol Microbiol Infect Dis. 2018;60:35-41. https://doi.org/10.1016/j.cimid.2018.09.013

46. Shaikh S, Fatima J, Shakil S, Rizvi SM, Kamal MA. Antibiotic resistance and extended spectrum beta-lactamases: Types, epidemiology and treatment. Saudi J Biol Sci. 2015;22(1):90-101. https://doi.org/10.1016/j.sjbs.2014.08.002

47. Mendonça J, Guedes C, Silva C, Sá S, Oliveira M, Accioly G, Baylina P, Barata P, Pereira C, Fernandes R. New CTX-M Group Conferring β-Lactam Resistance: A Compendium of Phylogenetic Insights from Biochemical, Molecular, and Structural Biology. Biology (Basel). 2022;11(2):256. https://doi.org/10.3390/biology11020256

48. Yu K, Huang Z, Xiao Y, Gao H, Bai X, Wang D. Global spread characteristics of CTX-M-type extended-spectrum β-lactamases: A genomic epidemiology analysis. Drug Resist Updat. 2024;73:101036. https://doi.org/10.1016/j.drup.2023.101036

49. Riccio ME, Verschuuren T, Conzelmann N, Martak D, Meunier A, Salamanca E, Musicha P. Household acquisition and transmission of extended-spectrum β-lactamase (ESBL) -producing Enterobacteriaceae after hospital discharge of ESBL-positive index patients. Clin Microbiol Infect. 2021;27(9),1322–1329. https://doi.org/10.1016/j.cmi.2020.12.024

50. Shastry BS. Role of SNP/haplotype map in gene discovery and drug development: An overview. Drug Dev Res. 2004;62(2),143–150. https://doi.org/10.1002/ddr.10377

51. Bonnet R. Growing group of extended-spectrum beta-lactamases: The CTX-M enzymes. Antimicrob Agents Chemother. 2004;48(1):1-14. https://doi.org/10.1128/AAC.48.1.1-14.2004

52. Garg S. Computational methods for chromosome-scale haplotype reconstruction. Genome Biol. 2021;22(1):101. https://doi.org/10.1186/s13059-021-02328-9

53. Lu S, Montoya M, Hu L, Neetu N, Sankaran B, Prasad BVV, Palzkill T. Mutagenesis and structural analysis reveal the CTX-M β-lactamase active site is optimized for cephalosporin catalysis and drug resistance. J Biol Chem. 2023;299(5):104630. https://doi.org/10.1016/j.jbc.2023.104630

54. Odey TOJ, Tanimowo WO, Afolabi KO, Jahid IK, Reuben RCl. Antimicrobial use and resistance in food animal production: Food safety and associated concerns in Sub-Saharan Africa. Int Microbiol. 2024;27:1–23. https://doi.org/10.1007/s10123-023-00462-x

55. Cisneros-Mayoral S, Graña-Miraglia L, Pérez-Morales D, Peña-Miller R, Fuentes-Hernández A. Evolutionary history and strength of selection determine the rate of antibiotic resistance adaptation. Mol Biol Evol. 2022;39(9):msac185. https://doi.org/10.1093/molbev/msac185

56. Koh XP, Shen Z, Woo CF, Yu Y, Lun HI, Cheung SW, Kwan JKC, Lau SCK. Genetic and ecological diversity of *Escherichia coli* and Cryptic Escherichia Clades in Subtropical Aquatic Environments. Front Microbiol. 2022;13:811755. https://doi.org/10.3389/fmicb.2022.811755

57. Judge A, Hu L, Sankaran B, Van Riper J, Venkataram Prasad BV, Palzkill T. Mapping the determinants of catalysis and substrate specificity of the antibiotic resistance enzyme CTX-M β-lactamase. Commun Biol. 2023;6(1):35.. https://doi.org/10.1038/s42003-023-04422-z

58. Egorov A, Rubtsova M, Grigorenko V, Uporov I, Veselovsky A. The role of the Ω-Loop in regulation of the catalytic activity of TEM-type β-lactamases. Biomolecules. 2019;9(12):854. https://doi.org/10.3390/biom9120854

59. Kumar P, Kayastha A, Singh VK, Kayastha AM. In silico structural and functional insight into the binding interactions of the modeled structure of watermelon

urease with urea. ACS Omega. 2023;9(2):2272-2285. https://doi.org/10.1021/acsomega.3c05993

60. Yang J, Zhang Y. Protein structure and function prediction using I-TASSER. Curr Protoc Bioinformatics. 2015;52:5.8.1-5.8.15. https://doi.org/10.1021/acsomega.8b00721

61. Sobolev OV, Afonine PV, Moriarty NW, Hekkelman ML, Joosten RP, Perrakis A, Adams PD. A Global ramachandran score identifies protein structures with unlikely stereochemistry. Structure. 2020;28(11):1249-1258.e2. https://doi.org/10.1016/j.str.2020.08.005

62. Wlodawer A. Stereochemistry and validation of macromolecular structures. Methods Mol Biol. 2017;1607:595-610. https://doi.org/10.1007/978-1-4939-7000-1_24

63. Mora-Lagares L, Minovski N, Caballero Alfonso AY, Benfenati E, Wellens S, Culot M, Gosselet F, Novič M. Homology modeling of the human p-glycoprotein (ABCB1) and insights into ligand binding through molecular docking studies. Int J Mol Sci. 2020;21(11):4058. PMC7312539. https://doi.org/10.3390/ijms21114058

64. Kim HY. Statistical notes for clinical researchers: Two-way analysis of variance (ANOVA)-exploring possible interaction between factors. Restor Dent Endod. 2014;39(2):143-7. http://dx.doi.org/10.5395/rde.2014.39.2.143

65. Ahmadvand P, Avillan JJ, Lewis JA, Call DR, Kang C. Characterization of interactions between CTX-M-15 and clavulanic acid, desfuroylceftiofur, ceftiofur, ampicillin, and nitrocefin. Int J Mol Sci. 2022;23(9):5229. https://doi.org/10.3390/ijms23095229

66. Yang KB, Cameranesi M, Gowder M, Martinez C, Shamovsky Y, Epshtein V, Hao Z, Nguyen T, Nirenstein E, Shamovsky I, Rasouly A, Nudler E. High-resolution landscape of an antibiotic binding site. Nature. 2023;622:180–187 https://doi.org/10.1038/s41586-023-06495-6

67. Tunstall T, Portelli S, Phelan J, Clark TG, Ascher DB, Furnham N. Combining structure and genomics t o understand antimicrobial resistance. Comput Struct Biotechnol J. 2020;18:3377-3394. https://doi.org/10.1016/j.csbj.2020.10.017

68. Glasgow A, Hobbs HT, Perry ZR, Wells ML, Marqusee S, Kortemme T. Ligand-specific changes in conformational flexibility mediate long-range allostery in the lac repressor. Nat Commun. 2023;14(1):1179. 2023;14(1):4208. https://doi.org/10.1038/s41467-023-36798-1

69. Shoeib NA, Al-Madboly LA, Ragab AE. In vitro and in silico β-lactamase inhibitory properties and phytochemical profile of Ocimum basilicum cultivated in central delta of Egypt. Pharm Biol. 2022;60(1):1969–80. https://doi.org/10.1080/13880209.2022.2127791.

70. Ahmed M, Maldonado AM, Durrant JD. From byte to bench to bedside: Molecular dynamics simulations and drug discovery. BMC Biol. 2023;21(1):299. https://doi.org/10.1186/s12915-023-01791-z